TU Delft

Delft University of Technology

Fatigue crack propagation simulation of orthotropic bridge deck based on extended finite element method

Gupta, Ravi Shankar; Xin, Haohui; Veljkovic, Milan

DOI
10.1016/j.prostr.2020.01.036

Publication date
2019

Document Version
Final published version

Published in
Procedia Structural Integrity

Citation (APA)
Gupta, R. S., Xin, H., & Veljkovic, M. (2019). Fatigue crack propagation simulation of orthotropic bridge deck based on extended finite element method. *Procedia Structural Integrity*, *22*, 283 - 290. https://doi.org/10.1016/j.prostr.2020.01.036

Important note
To cite this publication, please use the final published version (if applicable).
Please check the document version above.

Copyright
Other than for strictly personal use, it is not permitted to download, forward or distribute the text or part of it, without the consent of the author(s) and/or copyright holder(s), unless the work is under an open content license such as Creative Commons.

Takedown policy
Please contact us and provide details if you believe this document breaches copyrights.
We will remove access to the work immediately and investigate your claim.

This work is downloaded from Delft University of Technology.
For technical reasons the number of authors shown on this cover page is limited to a maximum of 10.

Available online at www.sciencedirect.com

ScienceDirect

Procedia Structural Integrity 22 (2019) 283–290

Structural Integrity Procedia

www.elsevier.com/locate/procedia

First International Symposium on Risk and Safety of Complex Structures and Components

Fatigue crack propagation simulation of orthotropic bridge deck based on extended finite element method

Ravi Shankar Gupta, Haohui Xin*, Milan Veljkovic

[1]*Faculty of Civil Engineering and Geosciences, Delft University of Technology, Delft, the Netherlands*
**Corresponding author: H.Xin@tudelft.nl*

Abstract

Orthotropic Steel Decks (OSDs) are widely used in various types of steel bridges due to its benefits of light weight, high load bearing capacity and speedy construction. However, fatigue remains as the predominant problem for OSDs. Many researchers have investigated fatigue issues of welded joints through experiments but is not a cost-effective solution. Therefore, it is necessary to combine experimental data with numerical approaches. Fracture mechanics approach has already shown its reliability and can be used to model and analyze fatigue crack propagation. In this paper, a numerical simulation is performed to predict the fatigue crack propagation using extended finite element method (XFEM). Two numerical models were considered namely CT-specimen and OSD, to evaluate the modelling efficiency. To verify the simulation, the results were compared with the experimental data. In predicting the fatigue crack propagation rate using two-dimensional CT-specimen, numerical results provided a good agreement with a maximum difference of 0.03% in the slope (m) and 1.48% in the intercept (C) of the power law equation. Furthermore, a simulation was performed on three-dimensional OSD structure to predict the fatigue crack growth.

© 2019 The Authors. Published by Elsevier B.V.
This is an open access article under the CC BY-NC-ND license (http://creativecommons.org/licenses/by-nc-nd/4.0/)
Peer-review under responsibility of the First International Symposium on Risk and Safety of Complex Structures and Components organizers

Keywords: Fatigue; XFEM; Crack propagation; Compact-Tension specimen, Orthotropic bridge deck.

2452-3216 © 2019 The Authors. Published by Elsevier B.V.
This is an open access article under the CC BY-NC-ND license (http://creativecommons.org/licenses/by-nc-nd/4.0/)
Peer-review under responsibility of the First International Symposium on Risk and Safety of Complex Structures and Components organizers
10.1016/j.prostr.2020.01.036

1. Introduction

Structural components are often found to fail even under stresses below the ultimate or the yield stresses in the presence of fatigue loading. The fatigue phenomenon is due to micro-cracks initiation, nucleation and gradually forms macro cracks; see for example (Xin & Veljkovic 2019). The macro cracks will propagate under cyclic loading. The conventional static strength analysis is not enough to predict service behaviour of steel structures. Therefore, over the past few decades many scientists and structural engineers have focussed their attention to fatigue fracture problems during designing and analysing structural components. Orthotropic steel decks (OSDs) are one of such typical structural components which suffered from fatigue problems. Over the past decades, although many improvements in all aspects of design, fabrication, inspection, and maintenance have been achieved for such bridge decks, fatigue is still a predominant problem, mostly because of the complexity of prediction methods. One of the critical fatigue details is the welded connection between the deck plate and the longitudinal stiffener due to direct wheel loading and local high stress ranges. However, performing only experiments may not lead to a cost-effective solution. Therefore, it is necessary to combine the experimental data with the numerical approaches and preferably assuming basic material properties to predict behaviour of critical details.

Methods based on fracture mechanics could be used to model and analyse the fatigue crack propagation and subsequent failure of the structure. These methods have already shown its reliability in the aerospace and automobile industry. The use of Linear Elastic Fracture Mechanics (LEFM) models has several advantages as it significantly reduces requirement of experiments. Furthermore, this method can predict the crack propagation till subsequent failure, which implies that the total fatigue life of the structure can be predicted for a certain crack length. Therefore, remaining lifetime predictions could be made for existing bridges (Nagy, De Backer, & Bogaert, 2012).

ABAQUS® provides an enriched feature, commonly referred as Extended Finite Element Method (XFEM) to model discontinuity independent to the finite element mesh. This removes the requirement of modelling domain and mesh to correspond to each other explicitly. Using XFEM, it is possible to evaluate automated crack propagation by arbitrarily inserting the crack into the existing model. The mesh around the crack tip should be sufficiently small to have to get accurate prediction which leads to high computational effort. Two options are available to model crack propagation, either by cohesive segment method or the linear elastic fracture mechanics (LEFM) approach in conjunction by phantom nodes (*Abaqus V. 6.14 Documentation*, 2014).

This paper focusses on numerical simulation of fatigue crack propagation using XFEM based on LEFM and virtual crack closure technique (VCCT). The first part deals with the fatigue crack propagation of a two-dimensional Compact-Tension (CT) specimen. To evaluate the efficiency of the assumed material parameters, the numerical results were compared with the results of the fatigue coupon tests (de Jesus et al., 2012). In the second part, a numerical simulation on fracture crack propagation of orthotropic steel deck (OSD) was performed to predict the fatigue crack growth. The results were validated against the beach marks measurement from the fatigue test (Nagy, 2016).

Nomenclature

a	Crack size
2c	Crack length
C, m	Material dependent parameters of the Paris Law
CT	Compact-Tension
C_3, C_4	Material constants based on fracture energy release rate
HAZ	Heat Affected Zone
IIW	International Institute of Welding
LEFM	Linear Elastic Fracture Mechanics
OSD	Orthotropic Steel Deck
RP	Reference Point ABAQUS®
ΔK	Stress Intensity Factor range
VCCT	Virtual Crack Closure Technique
XFEM	eXtended Finite Element Model

2. Fatigue crack propagation prediction of CT-specimen

2.1. XFEM model

2.1.1. Geometry

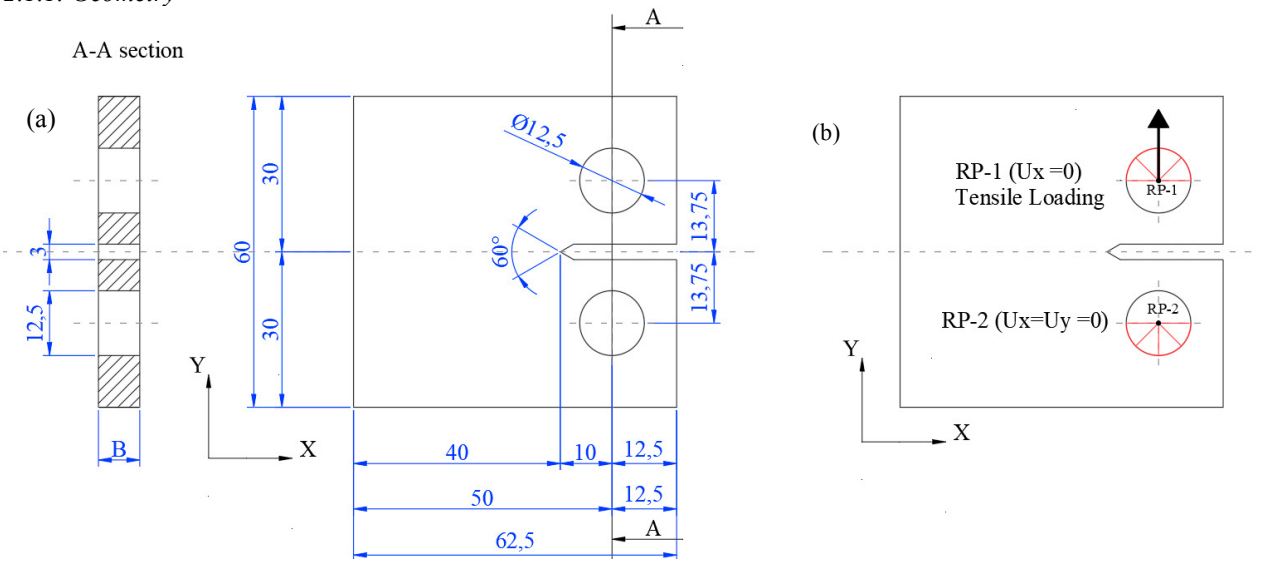

Figure 1 (a) Geometry and (b) Boundary conditions of CT-specimen (unit: mm)

A full scale two-dimensional XFEM-model was created based on the dimensions shown in Figure 1 (a) and the material properties were: Young's modulus E=210500 MPa and Poisson's ratio υ=0.3. In modelling the realistic boundary conditions of CT specimen, two reference points namely RP-1 and RP-2 were incorporated at the center of the holes which were coupled (kinematically constraint in all the direction for translation and rotation) with the two-interior half holes of the CT specimen. The boundary conditions were applied on these reference points as specified in Figure 1 (b). Crack domain represents the enrichment region contains a crack tip placed at the notch of the specimen illustrated in Figure 3 (a). The XFEM model consist of shell elements and was modelled using a 4-node bilinear plane stress quadrilateral with linear geometric order. The mesh size should be sufficiently small to capture accurate stresses near the crack tip. However, a numerical model with fine mesh can be time-consuming, therefore a variable mesh was used. In the enrichment area (crack propagation region) mesh size of 0.5 mm was adopted and 2 mm in the non-enrichment area was used, as shown in Figure 3(b).

2.1.2. LEFM implementation

Virtual Crack Closure Technique (VCCT) was used in the XFEM-based linear elastic fracture mechanics for crack propagation analysis by the direct cyclic approach with a time increment size of 0.05 per cycle. The crack growth is characterized by the Paris law, which relates the relative fracture energy release rates to fatigue crack growth rate (Figure 2). These fatigue crack growth rates are evaluated based on assigned VCCT technique. The crack propagation appears when the energy available for the crack is high enough to overcome the fracture resistance of the material. Since ABAQUS® analyses the fracture by the Griffith energy criterion approach, the Paris law parameters C_3 and C_4 were calculated assuming plane stress situation see equation (1) and (3) listed in Table 1. Material constants C_1 and C_2 which represents the onset of the fatigue crack growth were kept constant as 0.001 and 0 respectively equation (2).

$$\frac{da}{dN} = C\Delta K^m \quad (1)$$

$$f = \frac{N}{C_1 \Delta G^{C_2}} \geq 1.0 \quad (2)$$

$$\frac{da}{dN} = C_3 \Delta G^{C_4} \quad (3)$$

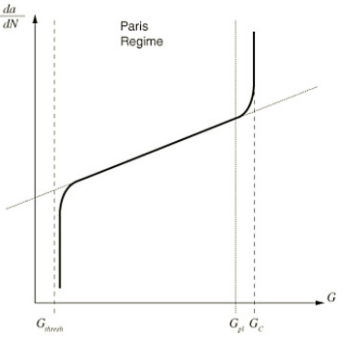

Figure 2 Fatigue crack growth (Abaqus V. 6.14 Documentation, 2014)

Table 1 Constants of Paris' Law and XFEM Abaqus.

R_σ	B *(mm)*	F_{max} *(N)*	F_{min} *(N)*	Experimental data		XFEM Abaqus	
				C^a	m	C_3	C_4
0.0	7.81	6118.6	61.8	2.5893E-15	3.5622	7.8419E-06	1.7811
0.25	7.47	7246.2	1811.5	2.5491E-15	3.7159	1.9790E-05	1.8579
0.50	7.41	9345.9	4672.9	8.2764E-16	3.8907	1.8768E-05	1.9453

Abaqus® provides three common mixed mode model for computing the equivalent fracture energy release rate G_{equivC} (*Abaqus V. 6.14 Documentation*, 2014). However, the choice of the model depending upon the analysis is not clear. In this study, Power law is selected for computing the equivalent fracture energy release rate represented in the equation (4) because of its simplicity in the relation of different modes of fracture.

$$\frac{G_{equiv}}{G_{equivC}} = \left(\frac{G_I}{G_{IC}}\right)^{a_m} + \left(\frac{G_{II}}{G_{IIC}}\right)^{a_n} + \left(\frac{G_{III}}{G_{IIIC}}\right)^{a_o} \quad (4)$$

The test results for the fracture toughness K_{IC} of the S355 steel grade obtained in the experiment (Bozkurt & Schmidová, 2018) using circumferentially cracked round bars (CCRB) ranges from 35.78 MPa√m to 40.4 MPa√m. This range can be possibly used in Compact-Tension (CT) specimen, a single edge notched bend or three-point loaded bend specimen, which is standardized by a different institution. Therefore, this data was taken as the base of this study and applied to the XFEM-model tabulated in Table 2.

Table 2 Critical energy release rate Gc

XFEM model	Critical energy release rate Gc			Exponent		
	Mode I	Mode II	Mode III	αm	αn	αo
CT- Specimen	6.5	6.5	6.5	1	1	1

2.2. Result and discussion

It has been observed the most critical element is completely fractured with a zero constraint and zero stiffness at the end of the stabilised cycle. As the enriched element is fractured, the load is redistributed, and a new fracture energy

release rate is computed for the enriched elements ahead of the crack tips for the next cycle. The fracture energy release rate was accounted for the enriched element ahead of the crack tip followed by the next enriched element when the previous enriched element is completely fractured. Simultaneously, the number of cycles was precisely noted as the fatigue crack propagated over the element length. An example of the XFEM output is illustrated in Figure 3 (b) representing the status of enriched element, the crack front and crack surface from the crack tip opening as STATUSXFEM, PHILSM and PSILSM output variable respectively at 1.87 x 10^5 cycles.

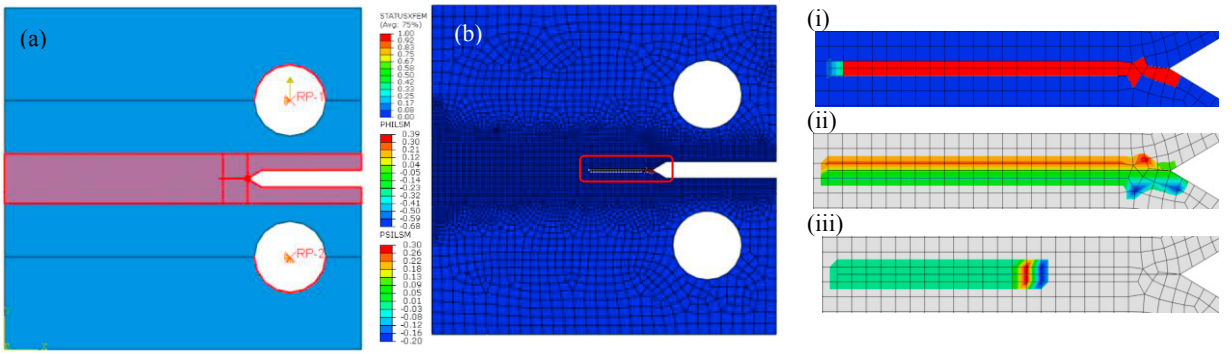

Figure 3 (a) XFEM model (b) Output results (i) STATUSXFEM (ii) PHILSM variable output (iii) PSILSM variable output

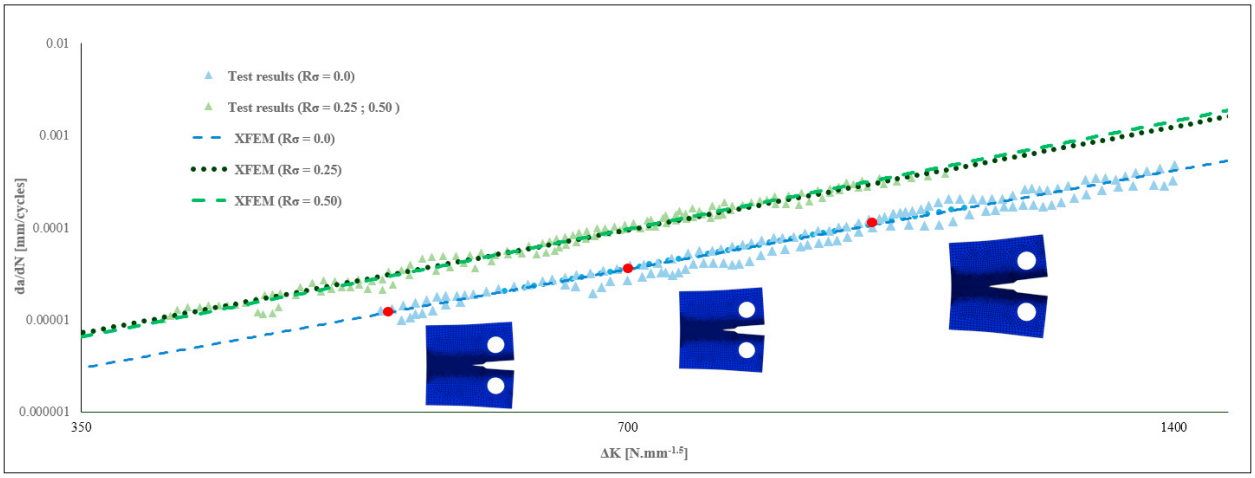

Figure 4 Fatigue crack propagation rates obtained from the numerical simulation compared with the test results

In Figure 4, the numerical prediction of the fatigue crack growth rate *da/dN* are plotted as a function of the stress intensity factor range ΔK in a log-log graph. The stress intensity factor values were computed in numerical simulation using the fracture energy-based criterion and the crack propagation rate was evaluated as the crack propagated along the length of the element starting from 15 mm as the initial crack size as shown in the Figure 3 (iii).

Comparing with different stress ratios, it was observed the rate of fatigue crack propagation is significantly increased as the stress ratio changes from 0 to higher positive values. This can be evaluated comparing the slopes of the curve. For stress ratios R=0.0, R=0.25 and R=0.50, the slopes were 3.56, 3.71 and 3.89 respectively. The slope difference is due to fatigue crack closure effects. Comparing with the experimental data, the simulated crack propagation provided good agreement with a maximum difference of 0.03% in the slope (m) and 1.48% in the intercept (C) of the power law equation.

3. Fatigue crack propagation prediction of OSD

3.1. XFEM model

3.1.1. Geometry

To numerically verify the fatigue crack propagation originating from the weld toe and propagating to the top of deck plate, a full scale XFEM-model was developed based on the dimensions and boundary conditions (Figure 5 (a)) with a length of 400 mm based on experiments reported by (Nagy, 2016). XFEM calculations are time-consuming and utilize a huge amount of computation power, the model was simplified. The XFEM model was created using shell and solid elements. The solid elements were used where the crack was considered, and the shell elements were used in the remaining part of the model. To ensure a rigid connection between these two parts, the edge surface of the shell was constrained to face region of the solids using shell-to-solid coupling. Since it is not possible to incorporate line-load in three-dimensional geometry in Abaqus®, a reference point (RP-1) was implemented which is kinematically coupled in all the directions to a straight line on the surface and the cyclic load is applied on that RP ranging from 0 KN to 31 KN.

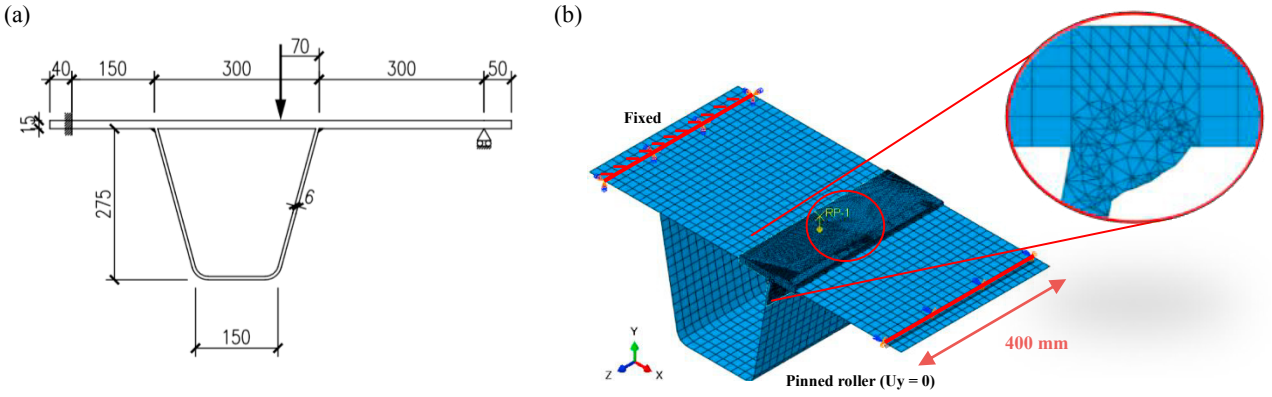

Figure 5 (a) Geometry of the OSD specimen (Nagy, 2016) (b) XFEM model: Boundary conditions and mesh quality

3.1.2. LEFM implementation

The material properties were: Young's modulus E= 210000 MPa and Poisson's υ=0.3. Virtual Crack Closure Technique (VCCT) was applied to the model XFEM-based linear elastic fracture mechanics for crack propagation analysis. A constant material fracture contact property was applied in the enrichment region. It is noted that the fatigue crack propagation rate is different for the base material, welds and HAZ zones. and the Paris constants can differ at such location. Same material property is assumed for a preliminary investigation in this paper. The material fracture property was implemented using Power law mix-mode behaviour illustrated in Table 3. Furthermore, the effect of residual stresses and micro-structure change will be further investigated in the future.

Table 3 Critical energy release rate Gc

XFEM model	C_3	C_4	Critical energy release rate G_c			Exponent		
			Mode I	Mode II	Mode III	αm	αn	αo
OSD	12.99E-06	1.5	11.9	11.9	11.9	1	1	1

While developing the XFEM model for automated crack propagation, some assumptions were made based on the fatigue experiment. Firstly, a semi-elliptical initial flaw was assumed shape with half-length a of 0.3 mm along the

minor axis and a half-length c of 0.6 mm along the major axis. Based on the fractographic results from the fatigue experiment, the size of the crack varies around 0.3 mm. The choice of the initial crack size heavily influences obtained results. Often, an initial crack length is chosen between 0.1 and 1 mm (De Backer, 2006). Since the longitudinal stiffener is welded from only one side to the weld, and even the level of penetration is questionable, the initial elliptical crack length can go up to 1mm and 0.5 mm in the longitudinal and transversal direction respectively (De Backer, 2006).Secondly, the crack is assumed to be originating from the center of the specimen. Therefore, the initial flaw was positioned at the weld toe perpendicular to the deck plate.

3.1.3. Mesh

3D tetrahedron elements are easily applicable to almost every structure and can be an ideal choice for complex structure. To alleviate the shear locking issue, high-order quadratic elements were used. Therefore, the enrichment region was modelled using a 10-node tetrahedron with quadratic geometrical order Figure 5 (b). Solids part (non-enrichment region) was modelled using an 8-node linear brick with reduced integration of an average mesh size of 5 mm whereas a 4-noded shell element of 10 mm of mesh size was adapted for the shell part. Meanwhile, the incompatibility mesh (interfaces between a tetrahedron and hexahedral) was automatically generated using tie-constraints.

3.2. Result and Discussion

Figure 6 display the output of automated XFEM simulation and crack growth mechanism. The crack initiating from the weld toe propagated in both longitudinal and vertical direction. As the shape of the initial flaw was assumed to be semi-elliptical, the growth followed almost in elliptical fashion. Figure 6 (a) displays the crack growth at different stage during fatigue crack propagation. The shape of fatigue crack propagated keeping the elliptical shape due to the use of tetrahedron elements the corresponding SIF distribution along the crack front.
Figure 6(d) displays the simulated crack front dimension after 2.20 x 10^5 cycles.

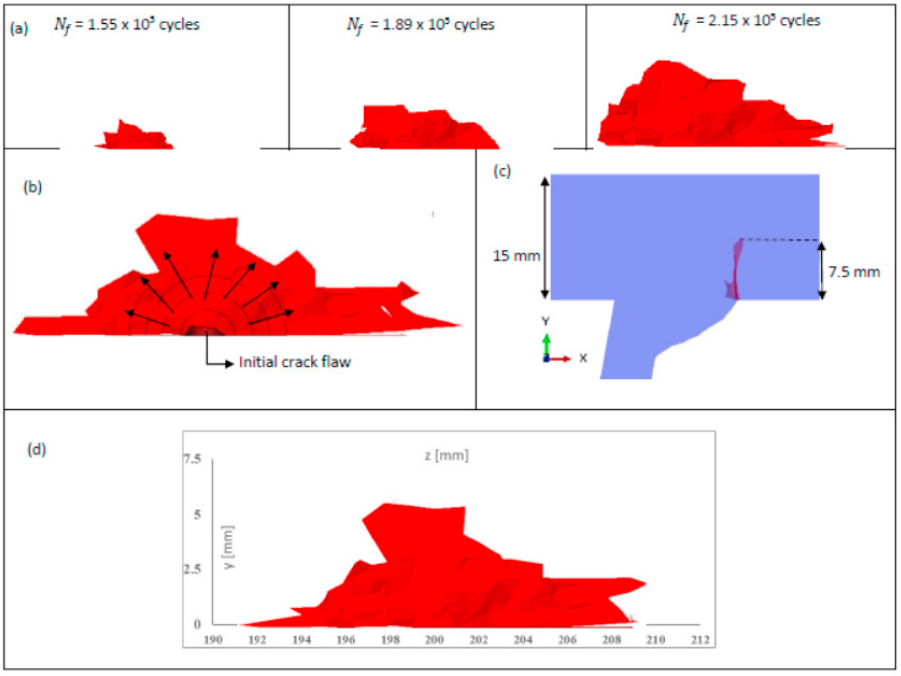

Figure 6 (a) Stages of crack propagation displayed as STATUSXFEM output (b) XFEM crack simulation including the initial semi-elliptical crack (c) Side view corresponding with the weld toe crack simulation (d) Crack front dimension

4. Conclusion

Modeling of a fatigue crack propagation using XFEM in a CT specimen and a segment of OSD is presented and following are conclusions:

- The Paris law implementation in ABAQUS® for material constant C_3 and C_4 were computed corresponding to the material constant C and m from the following relationship between strain energy release rate and stress intensity factor: C_4=m/2 and C_3=C.E*^{C4} where E*=E for plane stress condition and E*=E/ (1- υ^2) for plane strain condition. The assumed material parameters were validated using 2D compact tension specimens against the test results. It is noted that the material parameters and stress intensity factor distribution along the crack front need to be further investigated based on three-dimensional model.

- The simulation results of crack propagation rate of 2D shell XFEM CT-specimen showed a good agreement with the experimental results with a maximum difference of 0.03% in the slope (m) and 1.48% in the intercept (C) of the power law equation.

References

Abaqus V. 6.14 Documentation. (2014). (Vol. 651): Dassault Syst Simulia Corp.

Bignonnet, A., Carracilli, J. & Jacob, B. . (1991). ´ETUDE en FATIGUE des PONTS M´ETALLIQUES par un MOD`ELE de M´ECANIQUE de la RUPTURE. Retrieved from

Bozkurt, F., & Schmidová, E. (2018). Fracture Toughness Evaluation of S355 Steel Using Circumferentially Notched Round Bars.

De Backer, H. (2006). Optimalisatie van het vermoeiingsgedrag van het orthotrope brugdekconcept door verbeterde dispersie van de verkeersbelasting (in Dutch). (Phd thesis), Ghent University, Ghent, Belgium.

de Jesus, A. M. P., Matos, R., Fontoura, B. F. C., Rebelo, C., Simões da Silva, L., & Veljkovic, M. (2012). A comparison of the fatigue behavior between S355 and S690 steel grades. Journal of Constructional Steel Research, 79, 140-150. doi:https://doi.org/10.1016/j.jcsr.2012.07.021

Hobbacher. (2015). Recomendations for Fatigue Design of Welded Joints and Components. Retrieved from

Nagy, W. (2016). Fatigue assessment of orthotropic steel decks based on fracture mechanics. (dissertation), Ghent University, Ghent. (8602473)

Nagy, W., De Backer, H., & Bogaert, P. (2012). Crack propagation in a stiffener-to-deckplate connection of an orthotropic steel bridge deck.

Xin, H., & Veljkovic, M. (2019). Fatigue crack initiation prediction using phantom nodes-based extended finite element method for S355 and S690 steel grades. Engineering Fracture Mechanics. 214. 164-176